American Journal of Mechanical Engineering, 2016, Vol. 4, No. 7, 312-319
Available online at http://pubs.sciepub.com/ajme/4/7/15

DOI:10.12691/ajme-4-7-15

Fatigue Analysis of a Fire Truck Drop Tow Hitch for an O1 Category Water Pump Trailer

Cosmin Roszkos*, Jozef Bocko, Tomáš Kula

Faculty of Mechanical Engineering, Technical University of Košice, Košice, Slovakia
*Corresponding author: cosmin.roszkos@yahoo.com

Abstract This paper presents static and fatigue analyses of a fire truck drop tow hitch for an O1 category water pump trailer. In total 4 geometry variants with different features have been analyzed using the FEM. The loading forces have been calculated based on two different weights: the weight of the water pump trailer (the only trailer meant to be towed by the fire truck) and the category O1 gross trailer weight. Two different calculation methods were used: a calculation method recommended by the standard and a calculation method based on the physical breaking tests performed on the fire truck. The results of the performed analyses show the structural differences of the 4 geometry variants. The additional stiffening elements added to the base design have decreased the maximum deformation values, but the maximum stress and strain values have been raised especially in areas where stress concentrators are present.

Keywords: *drop tow hitch, fatigue life, finite element method, loading force, equivalent stress*

Cite This Article: Cosmin Roszkos, Jozef Bocko, and Tomáš Kula, "Fatigue Analysis of a Fire Truck Drop Tow Hitch for an O1 Category Water Pump Trailer." *American Journal of Mechanical Engineering*, vol. 4, no. 7 (2016): 312-319. doi: 10.12691/ajme-4-7-15.

1. Introduction

A tow hitch (or tow bar) is a device used to provide a connection between a towing vehicle and a trailer. A drop tow hitch fulfills the same role, but in this case the ball mount is located considerably lower than the towing vehicle's tow hitch receiver (Figure 1). Drop tow hitches must meet strict criteria because they represent a linkage between two moving vehicles and therefore they are safety relevant.

The load applied to a drop tow hitch is cyclic and not static. The repetition of a static load is dangerous, because as the number of load cycles increase, the allowed stress and strain levels decline. Stress values which are located below the yield stress value of the used materials can also lead to small plastic deformations, which in turn may cause the failure of the part or assembly [1,2].

The main focus of every manufacturer is to reduce the weight of their products, in other words, to use the smallest possible amount of material. The weight reduction of parts can't be obtained without detailed analyses, which include the fatigue analysis [3,4].

Because the main part of the designed drop tow hitch is a welded part, special attention has to be given to the joining areas, where welds are present. The fatigue analysis of welded structures can be analyzed by using different concepts: stress, strain or fracture mechanics. These linear-elastic principals require the weld geometry to be designed with a reference radius, in order to calculate the stress values and see if they fall below the permitted values [5-10]. The most preferred approach for different kind of welded constructions is the notch stress approach [11,12,13].

When designing parts for automobile vehicles, other aspects need to be considered as well. The drop tow hitch transmits energy to the vehicle's occupants through the vehicle's chassis therefore energy absorption should be taken into consideration as well when designing such a product [14,15]. In real situations however, there will always be a degree of uncertainty caused by unknown material properties, stress analysis errors, possible fabrication flaws, etc. In order to make the design as safe as possible, in this case a safety factor of 1.2-1.4 is desired [16].

2. Problem Description

The aim of this paper is to design and analyze a unique drop tow hitch for a fire truck and water pump trailer. The parts that are given and cannot be modified are the coupling ball with its mounting screws and the towing eyelet with its mounting screws. From the design point of view, the task was to develop the linkage between these two main parts, without modifying the chassis of the fire truck or trailer, which is prohibited due to legislative restrictions. The analysis will consist of applying a static load and afterwards a cyclic load to the geometry. The calculations were performed using the FEM.

A total of 4 geometry variants were designed (Table 1), which include different geometry modifications. The geometry variants were designed gradually, starting from a base variant. Every modification was performed with the purpose of improving the design, until the requirements

were fulfilled. An exploded view of the last variant is illustrated in Figure 1. The towing eyelet (1) and the tow ball (2) geometries are the same for every design.

In the V1 variant, the main part consisted of a 80x5 square profile welded in a T-like structure known as the ball mount (3). The eyelet was connected with bolts (4) to the ϕ60 mm pin (5), which passed through the ball mount (3) and welded on the exterior sides.

The tow ball was joined to the ball mount by screws (6). Variant V2 was upgraded by adding a 50x50x5 T profile beam (7). The T profile was welded to the pin and to the ball mount. In variant V3, a weight reduction was made, by thinning the pin to a diameter of ϕ40 mm and shortening the screws, which bind the tow ball to the ball mount. A gusset has also been added for stiffening purposes. In variant V4 two stiffening bars (8) were connected to the ball mount by screws and weldments, in order to minimize the movement of the drop tow hitch while the loading was applied.

The pin's geometry (5) was constructed together with the T-profile beam (7), in order to eliminate singularities which would occur in the area where they bind together and to simulate the presence of the weld material.

The same principle was applied to the ball mount. In the area, where the two square profiles meet, a concave shape was added in order to imitate the weld and eliminate possible singularities. Because of the shape of the root geometry has no significant effect on the stress which occurs in the weld area [13], special attention wasn't given to the modeling of the weld roots.

In this analysis the task was to obtain a design, which would have a high fatigue life, therefore only the elastic properties of the materials were used (Table 2). The SN curve is shown in Figure 2.

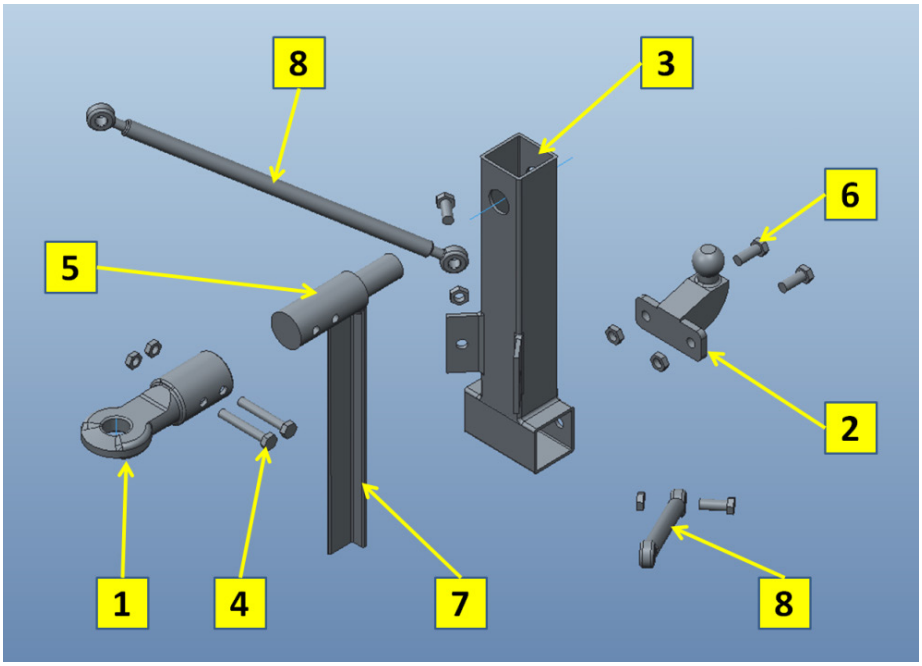

Figure 1. Exploded view of the V4 assembly

Table 1. Design variants

V1	V2	V3	V4
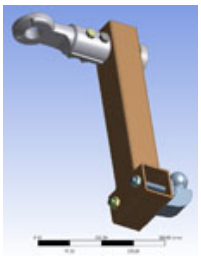	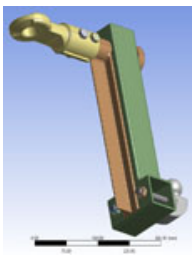	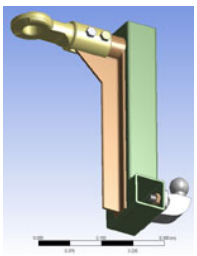	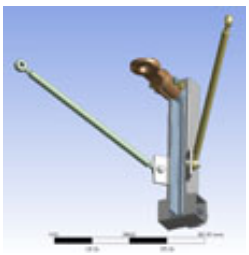
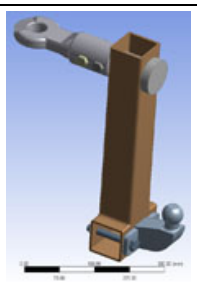		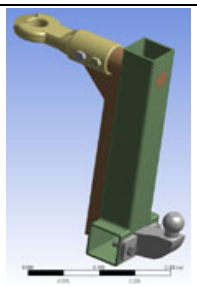	

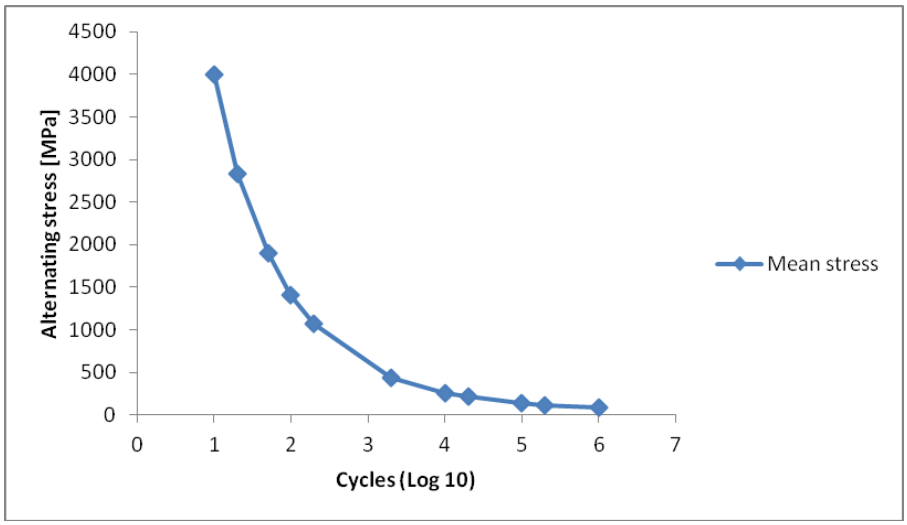

Figure 2. S-N curve of the applied material [17]

Table 2. Material properties [17]

	Quantity	Value
1	Density [kg/m^3]	7850
2	Young's modulus [MPa]	200 000
3	Poisson ratio [-]	0.3
4	Yield stress [MPa]	250
5	Ultimate strength [MPa]	460

2.1. Loading Force Calculation

As a basis for the structural simulations, two forces were used. One force was calculated using the weight of the truck, trailer and the gravitational force, as specified in the standard [18]. The other force was calculated using the measured deceleration of the truck while braking. The deceleration values obtained with the measurements made on the fire truck were higher than the values present in Maurya and Bokare's study [19].

2.1.1. Loading Force Calculation Recommended by the Standard

The longitudinal force between the towing vehicle and the trailer (D) is calculated using the following formula:

$$D = g \cdot \frac{m_M \cdot m_R}{m_M + m_R} \quad (1)$$

g is the gravitational acceleration, m_M is the total maximum calculated weight of the towing vehicle and m_R is the total maximum calculated weight of the towed vehicle.

The loading force (F_{res}) applied to the coupling device needs to be an alternative one and it needs to have amplitude of:

$$F_{res} = 0.6 \cdot D \pm 3\%. \quad (2)$$

The loading force must be applied in an almost sinusoidal manner.

2.1.2. Loading Force Calculation Using the Information from the Breaking Test

The deceleration was calculated using the initial speed, final speed and the distance needed to stop the vehicle. In this case the *work-energy principle* was used [20]. In other words, the change in the kinetic energy of an object is equal to the net work done by the object.

$$W = \frac{1}{2} m v_f^2 - \frac{1}{2} m v_i^2 \quad (3)$$

w is the total work done by the vehicle, m represents the weight of the vehicle, v_f is the final speed and v_i is the initial speed.

The energy done on the car in distance s has to be equal to its kinetic energy. Then by using:

$$W = F_d \cdot s \quad (4)$$

F_D is the force calculated from the deceleration and s is the total travelled distance of the vehicle. We can edit equation (3) and obtain the following formula:

$$F_d \cdot s = \frac{1}{2} m v_f^2. \quad (5)$$

The longitudinal force can now be calculated using one of the following formulas:

$$F_d = \frac{m v_f^2}{2s} \text{ or } F_d = \frac{m (v_2 - v_1)^2}{s_2 - s_1} \quad (6)$$

v_2 is the terminal speed, v_1 is the starting speed of the vehicle, s_2 is the end point of the travelled distance and s_1 is the starting point from where the measurement began (In the loading calculations, the average breaking distance was used).

The necessary information for the calculations is shown in the next table (Table 3).

Table 3. Input data

	Quantity	Value	Unit
1	g	9.81	m/s^2
2	m_M	11 000	kg
3	m_R	345 and 750	kg
4	v_1	13.88	m/s
5	v_2	0	m/s
6	s_1	0	m
7	s_2	9	m

Table 4. Loading forces

		Value	Unit		Quantity	Value	Unit	Trailer mass	Unit
L1	**Longitudinal forces**	3281.52	N	**Loading forces**	F_{res}	1969	N	345	kg
L2		3692.54	N		F_d	2216	N	345	kg
L3		6887.87	N		F_{res}	4133	N	750	kg
L4		8027.26	N		F_d	4816	N	750	kg

In order to verify if the drop tow hitch will withstand the loading of any trailer from the O1 category, it will be submitted to loadings calculated using a weight of 750kg (the maximum allowable weight for this category), besides the weight of the water pump trailer, for which it's intended for.

The forces calculated using the above mentioned methods are shown in Table 4. The difference between the loading forces calculated using the standard recommendation is slightly lower than the loading forces calculated from the breaking test information.

3. Boundary Conditions of the Simulations

The angles at which the loading is applied are determined by the distribution diagram of the loadings (Figure 3). This diagram was obtained from tests made on roads with different combinations of vehicles and trailers. To simplify the way the loading will be applied, the standard recommends two different angles, in order to keep in mind the vertical static loading and the dynamic loading.

In our case, only one angle was used. According to [18], because the horizontal axis that passes through the center of the towing ball is located lower than the horizontal axis that passes through the highest fixation point of the coupling device (reference line), the loading must be performed with an angle of $\alpha = 15° \pm 1°$ (Figure 4) [18].

The loading force was applied on the whole surface of the tow ball (Figure 5), because it's a back and forth movement. The force was applied in 5 steps, in order to be able to see the response of the model throughout the whole loading process.

The drop tow hitch was constrained only at the inner surface of the towing eyelet (Figure 5) by removing all degrees of freedom. To verify its structural stiffness, the movement of the inner surface of the drop tow hitch is totally restricted.

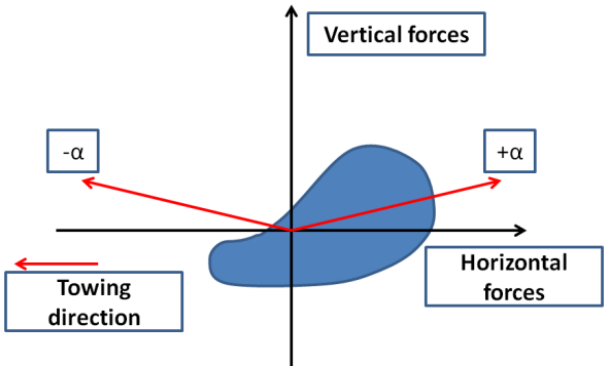

Figure 3. Distribution diagram of the loading forces [18]

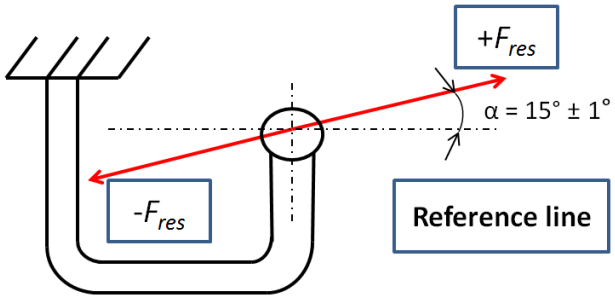

Figure 4. Load direction diagram [18]

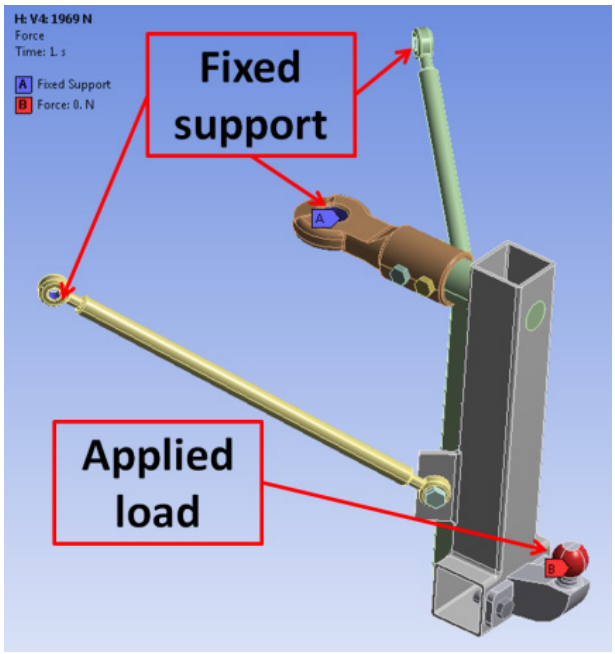

Figure 5. Boundary conditions

4. Results

In Table 5 the approximate maximum values of the equivalent von Mises stress, the approximate maximum equivalent strain values and the maximum deformation values are given.

In every variant, the maximum deformation occurred in the lower part, in the tow ball area (Figure 6 – Figure 9). The smallest deformation value was reached by variant V4 with the L1 load, followed by variant V3, variant V2 and variant V1. The smallest stress value was reached by the variant V1, with the L1 load (Figure 10 – Figure 13). The peak stress value on variant V1 arose on the bottom side of the weld that joins the pin to the ball mount. Stress concentrators also appeared on the other variants: on variant V2 and V4 at the tip weld between the T profile and pin; on variant V3 at the corner weld between the T

profile and the gusset plate. The equivalent strain evaluation has showed similar results to the equivalent stress results.

Table 5. Maximum stress, strain and deformation values

	Maximum equivalent von Mises stress [MPa]			
V1	72	81	160	184
V2	128	145	270	316
V3	76	86	144	168
V4	49	54	112	129
	Maximum equivalent strain [-]			
V1	0.0004	0.0004	0.0008	0.0009
V2	0.0006	0.0007	0.0013	0.0016
V3	0.0005	0.0005	0.0012	0.0013
V4	0.0002	0.0002	0.0005	0.0006
	Maximum deformation [mm]			
V1	7.9	8.5	13.3	14.6
V2	4.4	5	9.4	10
V3	5	5.6	9.5	10.8
V4	1.2	1.3	1.9	2.1
Load	**L1**	**L2**	**L3**	**L4**

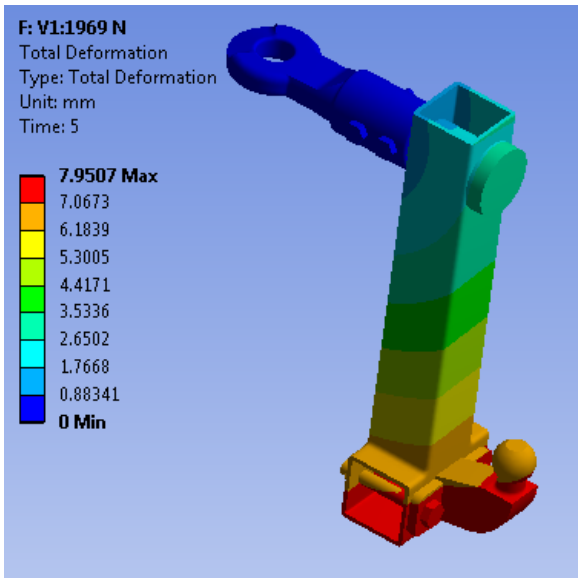

Figure 6. Total deformation plot – variant V1 (L1) [mm]

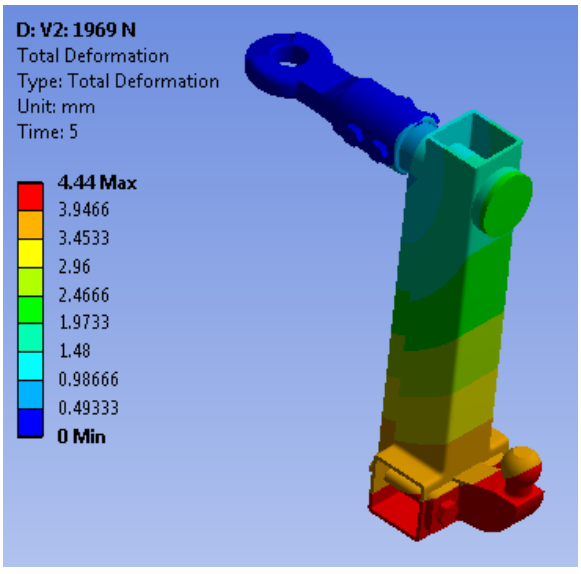

Figure 7. Total deformation plot – variant V2 (L1)[mm]

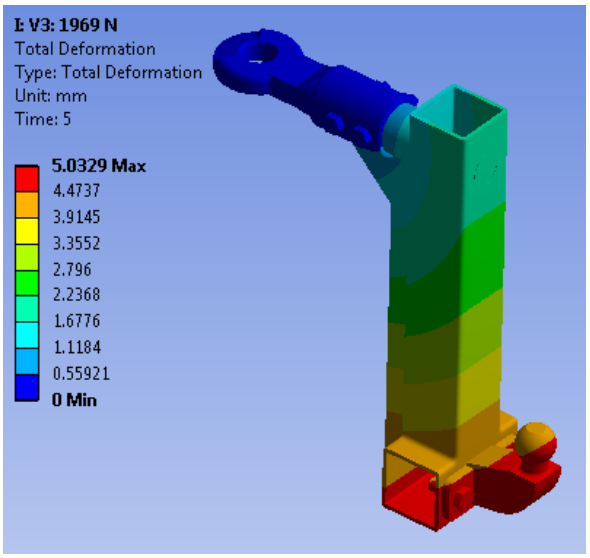

Figure 8. Total deformation plot – variant V3 (L1) [mm]

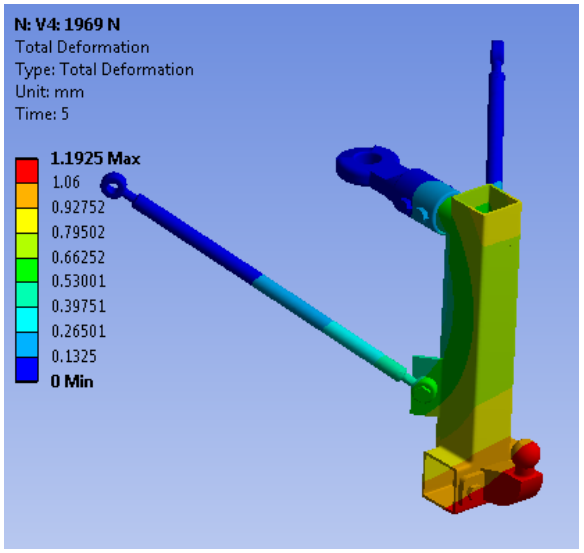

Figure 9. Total deformation plot – variant V4 (L1) [mm]

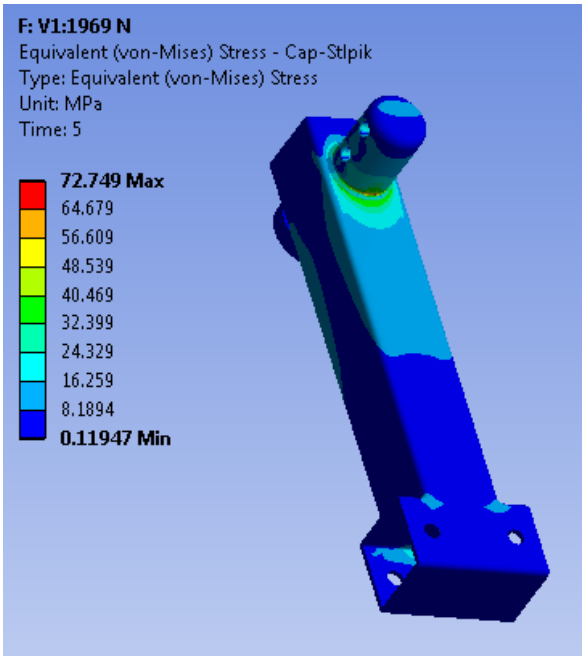

Figure 10. Equivalent von Mises stress plot – variant V1 (L1) [MPa]

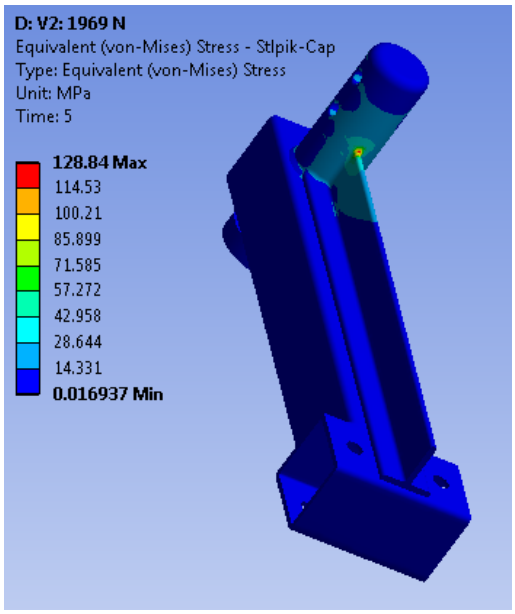

Figure 11. Equivalent von Mises stress plot – variant V2 (L1) [MPa]

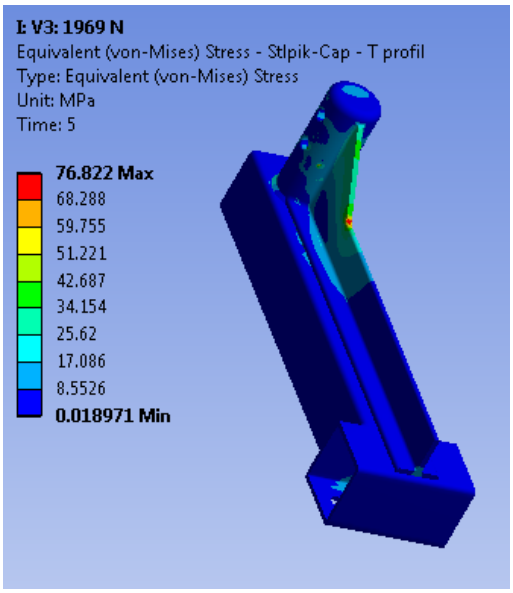

Figure 12. Equivalent von Mises stress plot – variant V3 (L1) [MPa]

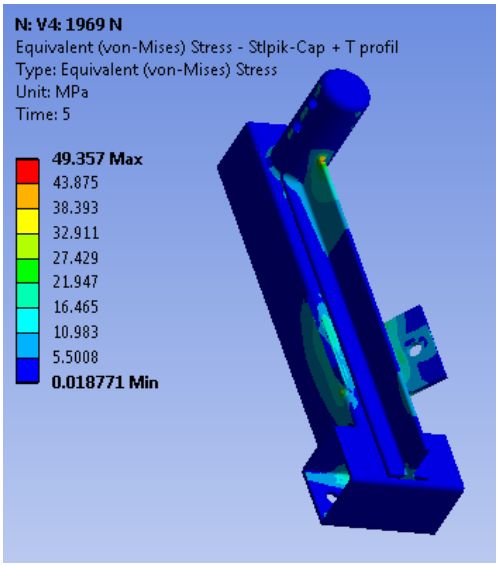

Figure 13. Equivalent von Mises stress plot – variant V4 (L1) [MPa]

Overall, the smaller loading forces obtained smaller maximum values, whilst with the larger loading forces, bigger values were reached.

The fatigue analyses were accomplished after finishing the static simulations, which were used as an input. As you can see in Table 6, the V1 and V4 variants have a fatigue life higher than $1*10^6$ cycles, when the L1 and L2 loadings were applied. The same result was reached with variant V3, but only when the L1 load was applied.

These results are consistent with the results obtained for the minimum factor of safety calculation. Only in the mentioned situations the minimum factor of safety was above the value of 1. From these only the V4 variant with the L1 and L2 loadings reached minimum factor of safety values above 1.2. The minimum factor of safety value is evaluated for a design life of $2*10^6$.

The fatigue life plots are shown from Figure 14 – Figure 17 and the minimum factor of safety plots from Figure 18 – Figure 21.

However, all mentioned values (maximum or minimum) are read from singularity points therefore the relevant values of the results are surpassing.

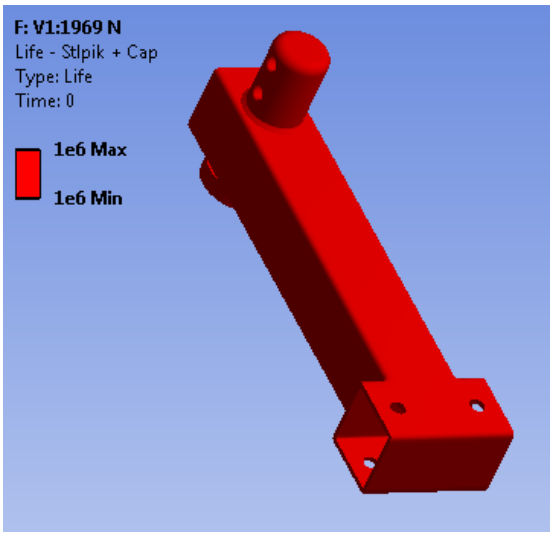

Figure 14. Fatigue life plot – variant V1 (L1) [cycles]

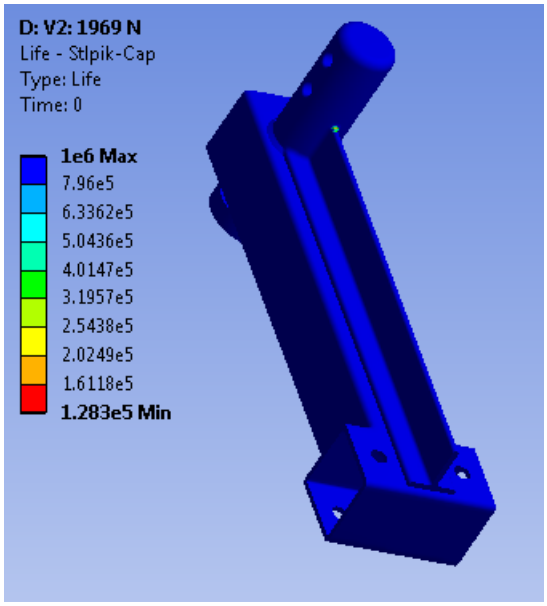

Figure 15. Fatigue life plot – variant V2 (L1) [cycles]

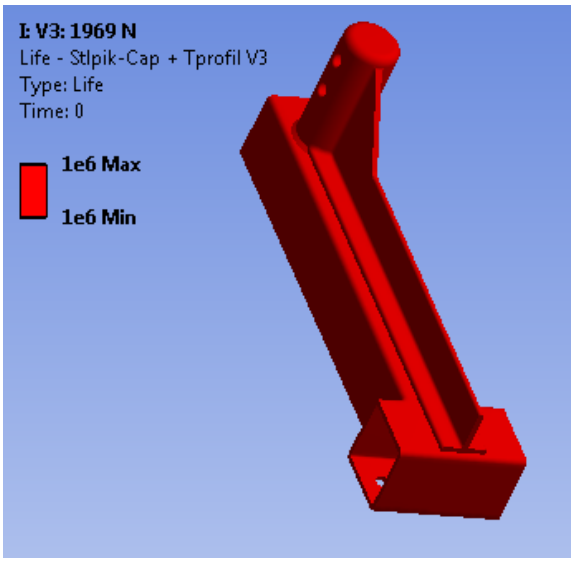

Figure 16. Fatigue life plot – variant V3 (L1) [cycles]

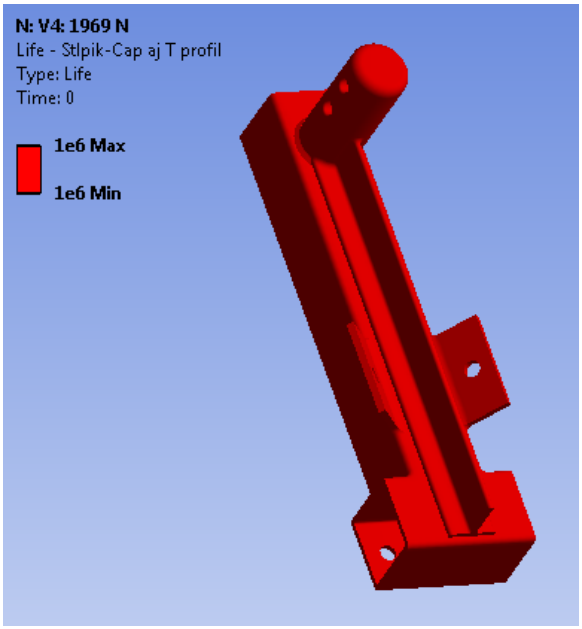

Figure 17. Fatigue life plot – variant V4 (L1) [cycles]

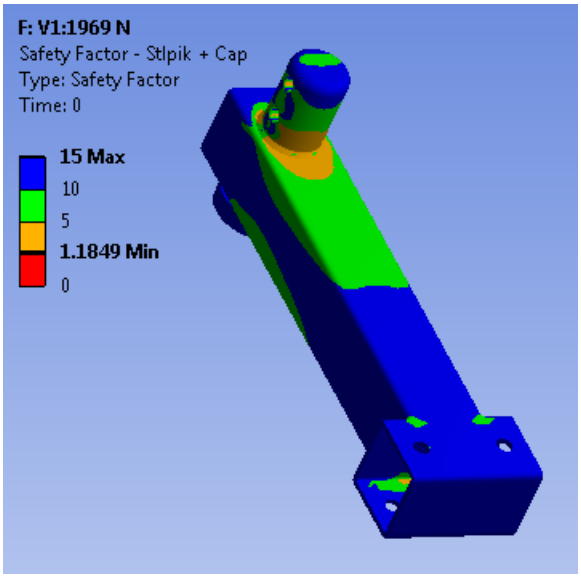

Figure 18. Safety factor plot – variant V1 (L1) [-]

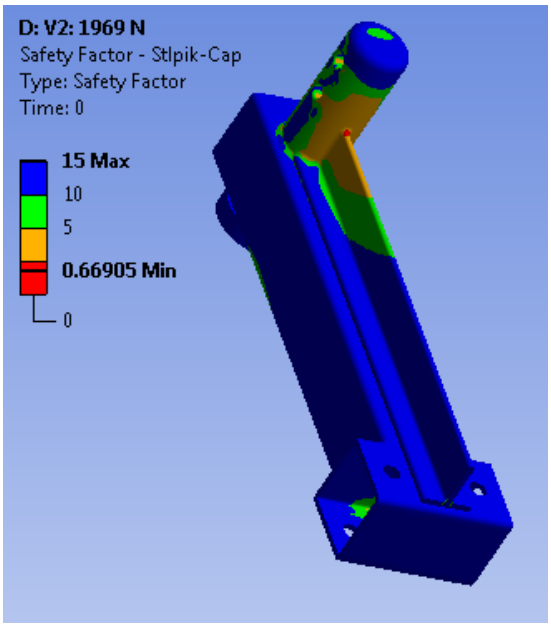

Figure 19. Safety factor plot – variant V1 (L1) [-]

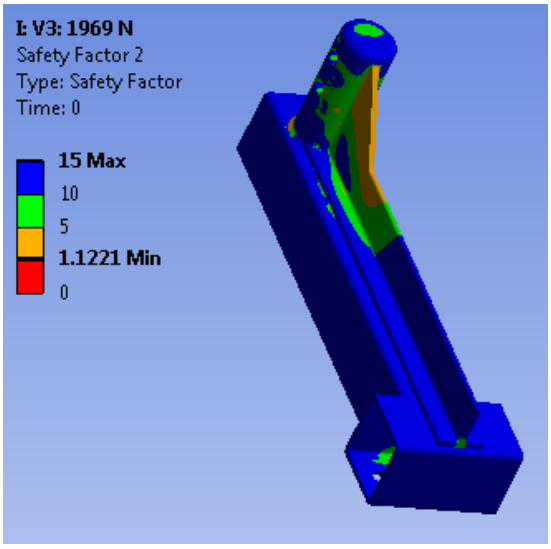

Figure 20. Safety factor plot – variant V1 (L1) [-]

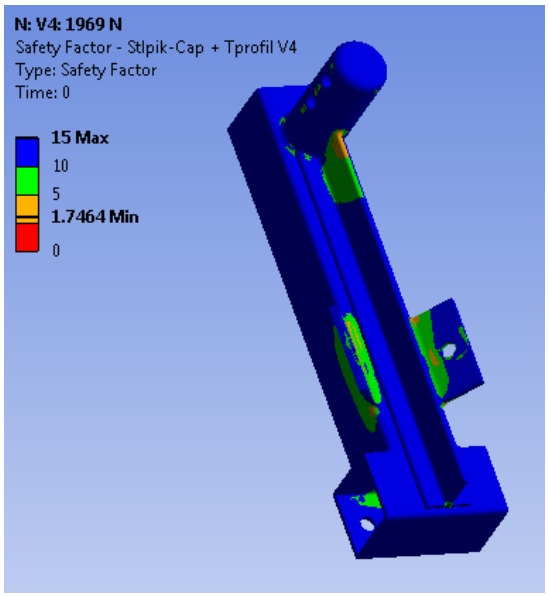

Figure 21. Safety factor plot – variant V1 (L1) [-]

Table 6. Minimum fatigue life and factor of safety values

	Fatigue life [cycles]			
V1	$1*10^6$	$1*10^6$	56830	34500
V2	$1.28*10^5$	83273	9011	5551
V3	$1*10^6$	$9.81*10^5$	22858	4995
V4	$1*10^6$	$1*10^6$	$2.16*10^5$	$1.24*10^5$
	Minimum factor of safety [-]			
V1	1.18	1.06	0.53	0.46
V2	0.66	0.59	0.31	0.27
V3	1.12	0.99	0.41	0.26
V4	1.74	1.59	0.76	0.66
Load	**L1**	**L2**	**L3**	**L4**

5. Conclusions

Four design variants of a drop tow hitch were designed and analysed using the FEM. The initial analyses consisted of static simulations. Because these kind of structures are prone to fatigue due to oscilating loads caused by the back and forth movement of the water pump trailer, the obtained results were used as an input for the fatigue analyses.

Four different loads were applied to the geometry variants. These loads were calculated using two different methods and two different maximum weights of the towed vehicle.

The main requirements were: a safety factor value which fits the 1.2-1.4 interval and a fatigue life of $2*10^6$ cycles [16,18]. The main task was to obtain a design which meets the requirements when the L1 and L2 loads are applied. The L3 and L4 loading was applied in order to check the performance of the design.

Variants V1, V3 and V4 reached a fatigue life above $1*10^6$ cycles with the L1 load and variants V1 and V4 reached the same fatigue life with the L2 load, but only variant V4 meets the safety factor requirement, which was evaluated for a design life of $2*10^6$ cycles.

The maximum stress and strain values appeared in welded areas. Although oval root geometry shapes were used to imitate real welds, singularity points have appeared in the areas, where the stress is higher. In other words, the used root geometries did not remove the singularity points. Stress concentrators however were highlighted by these high values.

The obtained results differ from the actual behaviour of the designs due to: singularity points, various residual stresses that arrose due to manufactoring reasons, like welding, tightening of screws and so on. These are only a few reasons, why an experiment is required to validate the results.

Acknowledgements

This research was supported by a grant from the Slovak Grant Agency VEGA No. 1/0731/16 - Development of Modern Numerical and Experimental Methods of Mechanical System Analysis.

References

[1] Bader, Q., Kadum, E., "Mean stress correction effects on the fatigue life behavior of steel alloys by using stress life approach theories," *International Journal of Engineering & Technology IJET-IJENS*, 14(04), 50-58, Aug. 2014.

[2] Kosteas, D., "*Fatigue behavior and analysis*," Talat lecture 2401, EAA – European Aluminium Association, 1994.

[3] Senthil, K.M., Vijayaragan, S., "Analytical and experimental studies on fatigue life prediction of steel and composite multi-leaf spring for light passenger vehicles using life data analysis," *Materials Science (Medžiagotyra)*, 13(2), 141-146, May 2007.

[4] Bhanage, A., Padmanabhan, K., "Design for fatigue and simulation of glass fiber/epoxy composite automobile leaf spring," *ARPN Journal of Engineering and Applied Sciences*, 9(3), 196-203, Mar. 2014.

[5] Sonsino, C.M., Fricke, W., de Bruyne, F., Hoppe, A., Ahmadi, A., Zhang, G., "Notch stress concepts for the fatigue assessment of welded joints – Background and applications," *International Journal of Fatigue*, 34, 2-16, May 2010.

[6] Park, W., Miki, C., "Fatigue assessment of large-size welded joints based on the effective notch stress approach," *International Journal of Fatigue*, 30, 1556-1568, Dec. 2007.

[7] Shen, W., Yan, R., Barltrop, N., Liu, E., Song, L., "a method of determining structural stress for fatigue strength evaluation of welded joints based on notch stress strength theory," *International Journal of Fatigue*, 90, 87-98, Apr. 2016.

[8] N'Diaye, A., Hariri, S., Pluvinage, G., Azari, Z., "Stress concentration factor analysis for welded, notched tubular T-joints under combined axial, bending and dynamic loading," *International Journal of Fatigue*, 31, 367-374, Aug. 2008.

[9] Radaj, D., Sonsino, C.M., Fricke, W., "Recent developments in local concepts of fatigue assessment of welded joints," *International Journal of Fatigue*, 31, 2-11, Jun. 2008.

[10] Thévenet, D., Ghanameh, M.F., Zeghoul, A., "Fatigue strength assessment of tubular welded joints by an alternative structural stress approach," *International Journal of Fatigue*, 51, 74-82, Feb. 2013.

[11] Fricke, W., Paetzold, H., "Full-scale fatigue tests of ship structures to validate the S-N curve approaches for fatigue strength assessment," *Marine Structures*, 23, 115-130, Jan. 2010.

[12] Fricke, W., von Lilienfeld-Toal, A., Paetzold, H., "Fatigue strength investigations of welded details of stiffened plate structures in steel ships," *International Journal of Fatigue*, 34, 17-26, Feb. 2011.

[13] Aygül, M., Al-Emrani, M., Urushadze, S., "Modeling and fatigue life assessment of orthotropic bridge deck details using FEM," *International Journal of Fatigue*, 40, 129-142, Dec. 2011.

[14] Agrawal, M.S., "Finite element analysis of truck chassis frame," *International Research Journal of Engineering and Technology (IRJET)*, 2(3), 1949-1956, Jun. 2015.

[15] Rahman, R.A., Tamin, M.N., Kurdi, O., "Stress analysis of heavy duty truck chassis as a preliminary data for its fatigue life prediction using FEM," *Jurnal Mekanikal*, 26, 76-58, Dec. 2008.

[16] Ullman, D.G., *The mechanical design process* - Second edition, The McGraw-Hill Companies Inc., Oregon, 314-324.

[17] Ansys version 16.2 Material database

[18] IRS ISO 3853: Jan. 1997, Road vehicle coupling device to tow caravans or light trailers- Mechanical strength test.

[19] Maurya, A.K., Bokare, P.A., "Study of deceleration behavior of different vehicle types," *International Journal for Traffic and Transport Engineering*, 2(3), 253-270, Jul. 2012.

[20] Camara, M., Bonanno, A., Sapia, P., "Revisiting work-energy theorem's implications," *European Journal of Physics*, 28, 1181-1187, Oct. 2007.